arXiv:1303.6822v1 [cond-mat.supr-con] 27 Mar 2013

Strong Pauli-limiting behavior and uniaxial pressure dependencies in KFe_2As_2

P. Burger,[1, 2] F. Hardy,[1] D. Aoki,[3, 4] A. E. Böhmer,[1, 2] R. Heid,[1] T. Wolf,[1] P. Schweiss,[1] R. Fromknecht,[1] M. J. Jackson,[5] C. Paulsen,[5] and C. Meingast[1]

[1] *Institut für Festkörperphysik, Karlsruher Institut für Technologie, 76021 Karlsruhe, Germany*
[2] *Fakultät für Physik, Karlsruher Institut für Technologie, 76131 Karlsruhe, Germany*
[3] *INAC, SPSMS, CEA Grenoble, 38054 Grenoble, France*
[4] *IMR, Tohoku University, Oarai, Ibaraki 311-1313, Japan*
[5] *Institut Néel, CNRS and Université Joseph Fourier, BP 166, 38042 Grenoble Cedex 9, France*

(Dated: March 28, 2013)

KFe_2As_2 single crystals are studied using specific-heat, high-resolution thermal-expansion, magnetization, and magnetostriction measurements. The magnetization and magnetostriction data provide clear evidence for strong Pauli limiting effects for magnetic fields parallel to the FeAs planes, suggesting that KFe_2As_2 may be a good candidate to search for the Fulde-Ferrell-Larkin-Ovchinnikov (FFLO) state. Using standard thermodynamic relations, the uniaxial pressure derivatives of the critical temperature (T_c), the normal-state Sommerfeld coefficient (γ_n), the normal-state susceptibility (χ), and the thermodynamic critical field (H_c) are calculated from our data. We find that the close relationship between doping and pressure as found in other Fe-based systems does not hold for KFe_2As_2.

PACS numbers: 74.70.Xa, 74.25.Bt, 74.62.Fj

The detailed understanding of Fe-based superconductors [1–4] continues to present a considerable challenge in condensed matter physics. Of particular interest recently has been the strongly hole doped compound KFe_2As_2 (K122), which is the end member of the $(Ba,K)Fe_2As_2$ system and has a much lower T_c of only 3.4 K [5, 6] than the optimal T_c value of about 40 K near 40% K content [7]. Whereas $Ba_{0.6}K_{0.4}Fe_2As_2$ appears to have a fully gapped *s*-wave order parameter [8, 9], there is strong evidence for a nodal superconducting state in K122. In fact, a *d*-wave state was predicted early on from functional renormalization group theory [10]. Experimentally, penetration depth and thermal conductivity studies have been interpreted in terms of a *d*-wave order parameter [11, 12], whereas recent laser angle-resolved photoemission (ARPES) experiments suggest a nodal *s*-wave state [13]. The electronic structure of K122 has been investigated both with de Haas-van Alphen (dHvA) and ARPES methods [14, 15], and these studies show that K122 has only hole pockets. This of course immediately raises the question of whether superconductivity in K122 has the same mechanism as the optimally doped system, for which superconductivity has been suggested to originate from interband pairing between electron and hole pockets [4]. Inelastic neutron scattering results still show signs of spin fluctuations, which are however incommensurate but may nevertheless lead to superconducting pairing in the heavily overdoped region [16, 17]. Paradoxically, K122 has the largest γ_n in the $(Ba,K)Fe_2As_2$ system in spite of the low T_c value, and this has been linked to a close proximity to an orbitally-selective Mott transition due to strong Hund correlations [18, 19].

In this Letter we study the normal- and superconducting-state properties of K122 using several thermodynamic probes: specific-heat, high-resolution thermal-expansion, magnetization, and magnetostriction measurements. Our magnetization and magnetostriction data clearly show that K122 is strongly Pauli limited for fields parallel to the FeAs planes and, thus, this system may be another possible candidate to search for the Fulde-Ferrell-Larkin-Ovchinnikov (FFLO) state. Using standard thermodynamic relations, the uniaxial pressure derivatives of the critical temperature (T_c), the normal-state Sommerfeld coefficient (γ_n), the normal-state magnetic susceptibility (χ), and the thermodynamic critical field (H_c) are calculated from our data. First, we find that the relative pressure derivatives of T_c are very anisotropic and of opposite sign as for Co-doped Ba122 [20]. For hydrostatic pressure, we find that both T_c and γ_n decrease. This is in contrast to the doping induced behavior and shows that pressure and doping can not be equated, as they can in the Co- and P-doped Ba122 systems [21, 22].

Single crystals of KFe_2As_2 were grown in alumina crucibles using a K-As rich flux. The crucibles were sealed in an iron cylinder filled with argon gas. After heating up to 980 °C the furnace was cooled down slowly at a rate of about 0.5 °C/h. Crystals with dimensions up to 3.0 × 2.5 × 1.0 mm^3 were used in the present investigation. The specific heat was measured with a commercial Quantum Design Physical Property Measurement System (PPMS) for $T > 0.4$ K and with a home-made calorimeter for $T < 0.4$ K. For $T > 2$ K, we used a vibrating sample magnetometer to measure the magnetization. For $T < 2$ K, magnetization measurements were performed using a low-temperature superconducting quantum interference device (SQUID magnetometer) equipped with a miniature dilution refrigerator developed at the Institut Néel-CNRS Grenoble. The sample was attached to a copper tress suspended from the dilution unit's mixing chamber which descends through the bore of the magnet. The magnetometer is equipped with a solenoid capable of producing fields up to 8 T. The setup can measure absolute values of the magnetization by the extraction method at temperatures down to 75 mK. The thermal expansion and the magnetostriction were measured in a custom-made capacitive dilatometer with a typical resolution of $\Delta L/L_0 \sim 10^{-8}$-$10^{-10}$ [21, 23].

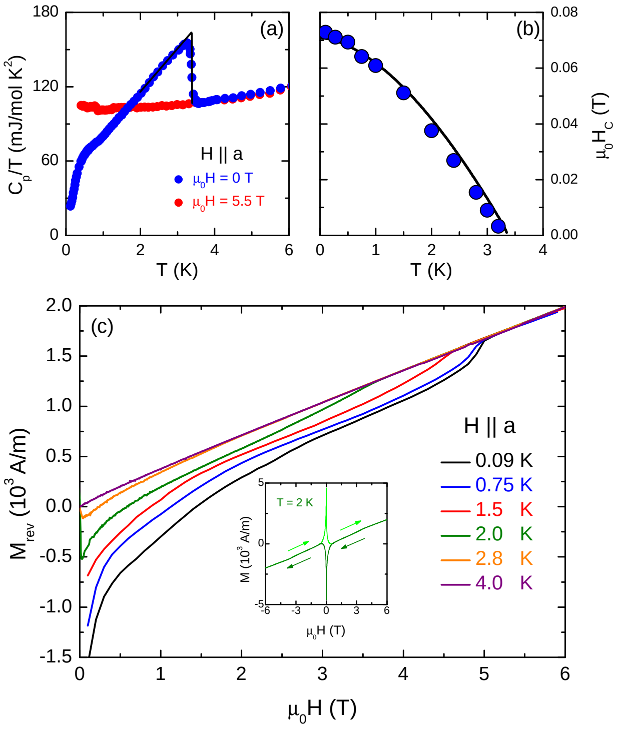

FIG. 1. (Color Online) (a) Specific heat of KFe_2As_2 in 0 and 5.5 T. (b) Thermodynamic critical field derived from specific-heat (line) and magnetization (symbol) measurements. (c) Reversible magnetization as a function of magnetic field. The inset shows the total magnetization at 2 K.

Fig.1(a) shows typical heat capacity data of our samples, clearly demonstrating a sharp superconducting transition and evidence for multigap behavior [24, 25]. We attribute the decrease of C_p/T below about 0.5 K to small superconducting gaps on parts of the Fermi surface, which surprisingly appear to be absent in some recent data [26]. In the following, we demonstrate that the thermodynamic critical field H_c obtained from the heat capacity data matches that obtained by our reversible magnetization measurements (see Fig.1(b)) quite well, which demonstrates that the heat capacity is not contaminated by any spurious magnetic contributions [26, 27]. H_c can be determined directly from the heat capacity using

$$E_{cond} = -\frac{1}{2}\mu_0 H_c^2 = \int_0^{T_c} (S_s - S_n)dT, \qquad (1)$$

where E_{cond} is the Cooper-pairs condensation energy while S_n and S_s are the normal- and superconducting-state entropies, respectively. We find $H_c(T = 0\text{ K}) = 0.072$ T. As shown in the inset of Fig.1(c), the magnetization is fully reversible for increasing and decreasing fields, except for a small region near zero fields. In order to eliminate this small hysteresis, the data were averaged for increasing and decreasing field, which yields reversible magnetization curves shown in Fig.1(c). The data show clear signs of Pauli paramagnetic behavior in both the normal and the superconducting state near H_{c2} at low temperatures. This is clearly seen in Fig.1(c) as an abrupt increase in $M(H)$ near H_{c2} instead of the usual Ginzburg-Landau linear dependence. The Pauli-limiting behavior will be discussed in more detail later. On the other hand, $H_c(T)$ can also be obtained by integration of the reversible magnetization using

$$\int_0^{H_{c2}} (M_s - M_n)dH = -\frac{H_c^2}{2}, \qquad (2)$$

where M_n and M_s are the reversible magnetization in the normal and superconducting states, respectively. The resulting values of H_c (shown in Fig.1(b)) agree quite well with those calculated from the heat capacity, demonstrating the overall consistency between our thermodynamic measurements.

We now discuss the strong Pauli-limiting behavior seen in our magnetization data (see Fig.1(c)). The shapes of both the reversible magnetization and the magnetostriction data shown in Fig.3 for H parallel to a at low temperatures point to a crossover to strong Pauli-limiting behavior [28]. The Pauli-limiting field for a singlet superconductor is given by [29]

$$H_p = \sqrt{\frac{1}{\chi}}H_c, \qquad (3)$$

which we can directly calculate from our specific-heat and magnetization data [18]. Thus, in the single-band approximation, we find crude values $H_p = 3.5$ T and 3.9 T for H parallel a and c, respectively. Since $H_p < H_{c2} = 5.1$ T only for H parallel a, strong Pauli depairing effects are expected only in this direction. Moreover, the weak pinning and the observation of quantum oscillations in these samples indicate that they are in the clean limit [30]. Thus, this strong paramagnetic behavior makes K122 a good candidate for seeking a possible FFLO state. From our magnetization data it is not clear whether the transition at H_{c2} really becomes first-order. More detailed low-temperature measurements and discussions will be presented elsewhere [30, 31].

We also performed thermal expansion and magnetostriction measurements in order to study the effects of pressure, in particular uniaxial pressure, on the superconducting and normal state properties of K122. Clear anomalies in the relative length changes, $\Delta L/L_0$, for the crystallographic a and c directions are seen at $T_c(H = 0\text{ T}) = 3.4$ K as shown in Fig.2(a) and (b). The red curves indicate the normal-state behavior, where superconductivity has been suppressed by a field of $H = 6$ T applied along the a-axis, and the dashed lines indicate the extrapolated behavior down to $T = 0$ K. From these data, it is clearly seen that superconductivity favors a longer (shorter) a-axis (c-axis). Fig.2(c) - (f) show the corresponding uniaxial thermal-expansion coefficients $\alpha = (1/L_i)dL_i/dT$ $(i = a, c)$, divided by temperature at different applied magnetic fields along the a-axis ((c) and (d)) and the c-axis ((e) and (f)). The anomalies at T_c have a clear step-like shape, indicating second-order transitions and decrease in temperature with increasing magnetic field. A small anomalous increase in the size of the expansivity anomaly is seen at 3.5 T in Fig.2(d); this is related to the strong Pauli-limiting for H parallel to a seen in the magnetization data.

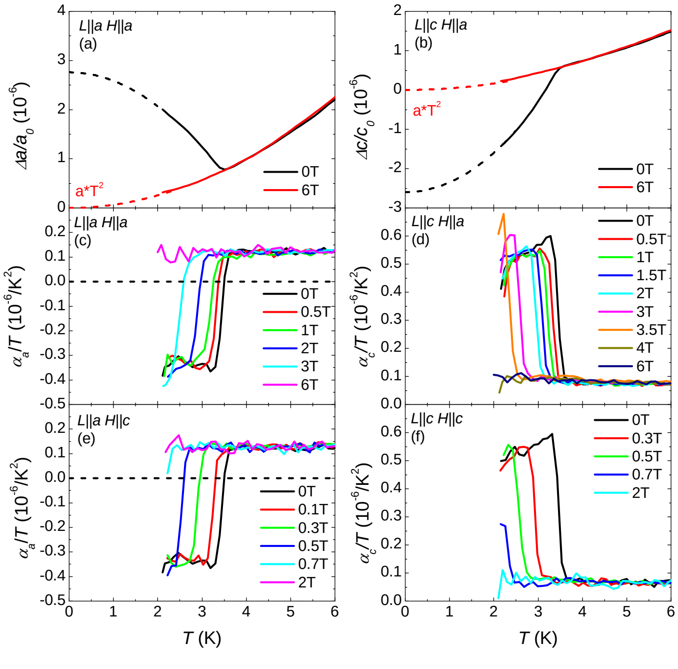

FIG. 2. (Color Online) (a) Relative length change of the a-axis (b) and c-axis in the normal (red curves) and the superconducting state (black curves). (c) - (f) Uniaxial thermal-expansion coefficients divided by temperature $\alpha_{a,c}/T$ as a function of temperature for both crystallographic axes and different fields.

In Fig.2 (c) - (f) we have plotted α/T versus temperature for the crystallographic a and c axes respectively showing a constant α/T value above the transition temperature, as one expects for a Fermi liquid. Using Maxwell relations this value is related to the pressure dependence of γ_n [21]:

$$\frac{\alpha_i}{T} = -\frac{1}{V}\frac{\partial(\frac{S}{T})}{\partial p_i} = -\frac{1}{V_m}\frac{d\gamma_n}{dp_i}(i = a, c). \tag{4}$$

The normal-state values of α/T are $\alpha_a/T = 0.12 \times 10^{-6}\mathrm{K}^{-2}$ and $\alpha_c/T = 0.08 \times 10^{-6}\mathrm{K}^{-2}$ which yield the following uniaxial-pressure dependencies of the normal-state Sommerfeld coefficients $d\gamma_n/dp_a = -7.74$ mJ mol^{-1}K^{-2}GPa^{-1} and $d\gamma_n/dp_c = -4.81$ mJ mol^{-1}K^{-2}GPa^{-1}.

In order to determine the uniaxial-pressure dependencies of T_c, we use the Ehrenfest relation [20, 32]:

$$\frac{dT_c}{dp_i} = \frac{\Delta\alpha_i V_m}{\Delta C_p/T_c}(i = a, c). \tag{5}$$

Here $\Delta\alpha_i$ is the jump in the thermal expansion along the i direction, $V_m = 61.27$ cm^3/mol^{-1} is the molar volume and ΔC_p is the specific heat jump. Using our values for the thermal-expansion ($\Delta\alpha_a = -1.68 \times 10^{-6}\mathrm{K}^{-1}$ and $\Delta\alpha_c = 1.85 \times 10^{-6}\mathrm{K}^{-1}$) and heat-capacity ($\Delta C_p/T_c = 54$ mJ mol^{-1}K^{-2}) [18] jumps from Fig.1(a), we find $dT_c/dp_a = -1.92$ K GPa^{-1} and $dT_c/dp_c = 2.10$ K GPa^{-1}. Our results show that the pressure dependence of T_c in KFe$_2$As$_2$ is very anisotropic. Indeed it is negative along the a-axis and positive along the c-axis, although the magnitudes are comparable. Interestingly as in Co- and P-doped Ba122 [20, 22], superconductivity couples strongly to the c/a ratio, but with opposite sign, i.e. a smaller, rather than a larger, c/a ratio enhances T_c. Under hydrostatic conditions we get a negative $dT_c/dp_{vol} = 2dT_c/dp_a + dT_c/dp_c = -1.74$ K GPa^{-1}. Our results are in qualitative agreement with the recent data of Bud'ko et al. [33], who find $dT_c/dp_{vol} = -1.0$ K GPa^{-1}, $dT_c/dp_a \approx -1.1$ K GPa^{-1} and $dT_c/dp_c \approx 1.1$ K GPa^{-1} from hydrostatic pressure and c-axis thermal expansion data.

The pressure dependence of the thermodynamic critical field at $T = 0$ K can be calculated using the following relation [34]:

$$\frac{\Delta L_i}{L_i} = \frac{L_{n,i} - L_{s,i}}{L_{s,i}} = \mu_0 H_c\left(\frac{dH_c}{dp_i}\right)(i = a, c) \tag{6}$$

where $\Delta L_i/L_i$ are the relative length changes from Fig.1. We obtain $dH_c^a/dp_a = -0.049$ T GPa^{-1} and $dH_c^a/dp_c = 0.046$ T GPa^{-1}.

Additional information about how uniaxial pressure affects the properties of K122 can be obtained from magnetostriction measurements (see Fig.3). The magnetostriction coefficient λ is directly related to the uniaxial pressure dependence of the magnetization via

$$\lambda_i = \frac{1}{L_i}\frac{dL_i}{dH} = -\frac{dM}{dp_i}(i = a, c). \tag{7}$$

Fig.3 shows the magnetostriction data for various sample and field orientations for temperatures between 1.7 K and 4 K. The pressure dependence of the normal-state Pauli paramagnetic susceptibility can be directly obtained from $\lambda(H)$, which also varies linearly with field strength (see Fig.3(c), (d), (g), (h)) from equation 7. With this we extract $d\chi^a/dp_a = -1.43 \times 10^{-5}\text{GPa}^{-1}$, $d\chi^c/dp_a = 4.13 \times 10^{-6}\text{GPa}^{-1}$, $d\chi^a/dp_c = -6.74 \times 10^{-6}\text{GPa}^{-1}$, and $d\chi^c/dp_c = -3.08 \times 10^{-5}\text{GPa}^{-1}$. Interestingly, the biggest effects of pressure on the magnetic susceptibility occur when the applied magnetic field is parallel to the measured direction and is one magnitude weaker for different orientations.

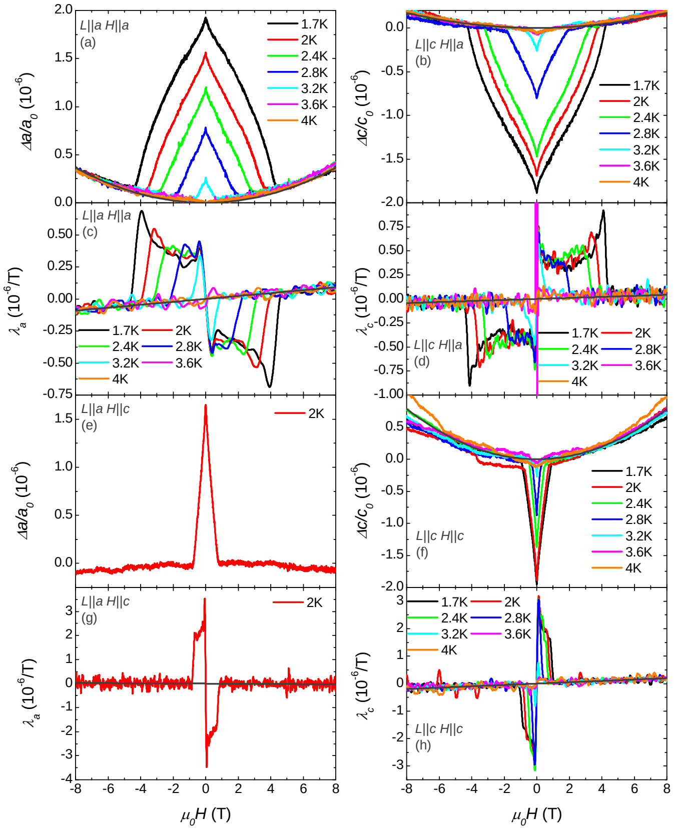

FIG. 3. (Color Online) Relative length changes and magnetostriction coefficients for the a-axis (left side) and the c-axis (right side) at different field directions.

The magnetostriction below T_c is fully reversible and thus, also provides information about how the reversible magnetization responds to uniaxial pressure [35, 36]. The reversible magnetostriction depends basically on two parameters, H_c and the Ginzburg-Landau parameter κ, which both can be pressure dependent. From the shape of $\lambda(H)$, it is evident that the main contribution to the magnetostriction comes from dH_c/dp_i and not from $d\kappa/dp_i$ [36] for both field directions. If $d\kappa/dp_i$ would be large, $\lambda(H)$ would change sign near $H_{c2}/2$. For $H \parallel a$, there is a strong increase in the size of the λ anomaly with decreasing temperatures, again pointing to the strong Pauli-limiting behavior.

A summary of the uniaxial pressure derivatives is given in table I; here we have also included the relative pressure derivatives, which allows us to directly compare the magnitude of the various derivatives. The largest relative pressure derivatives are for T_c and H_c, which are roughly equal both in magnitude and sign. Thus, the critical temperature and the condensation energy are strongly linked, which is not surprising. On the other hand, the relative pressure derivative of γ_n and χ are much smaller than those of T_c and H_c. Also, there is no direct correlation between the signs of dT_c/dp_i and $d\gamma_n/dp_i$, which implies that these quantities are not directly related. Here it is worth pointing out that pressure and doping are strongly correlated in Co- and P-doped systems [21, 22], which manifests itself in a similar dependence of T_c and γ_n versus either doping or pressure. Such a correlation between doping and pressure does not appear to work for the K-doped system. γ_n is largest and T_c is lowest for K122 and thus, if a similar equivalence would hold, one would expect that under hydrostatic pressure γ_n would increase since T_c decreases, which is the opposite of the observed behavior (see table I). Using a bulk elastic modulus from the DFT calculation of $B = 45$ GPa [37], we can also calculate volume Grüneisen parameters of the various physical quantities (see table I). Interestingly, these volume Grüneisen parameters of T_c and γ_n are of similar magnitude and sign as found in various U-based heavy fermion materials [38], which was interpreted in terms of a negative pressure dependence of the pairing interaction. Similar physics may be operating in K122, which may be considered a 3d-heavy-fermion metal [18].

In conclusion, the present thermodynamic investigation of K122 has revealed several interesting results. Clear evidence for strong Pauli H_{c2} limiting behavior is observed in the low temperature magnetization measurements. Further detailed studies are needed to determine if the low-temperature transition is truly first-order and for searching for other ordering phenomena, such as the elusive FLLO state. Interestingly, the derived uniaxial pressure derivatives show that superconductivity in K122 responds strongly to the c/a ratio of the lattice constants, but with the opposite sign as in Co- and P-doped Ba122, showing that this is not a universal characteristic of the pnictides. It is hoped that the various pressure derivatives derived here will add a stringent constraint on superconducting theories of this interesting low-T_c end compound.

The authors thank J. Schmalian, I. Vekhter, K. Grube, and D. Zocco for helpful discussions. This work has been supported by the DFG through SPP1458. The work performed in Grenoble was supported by the French ANR Projects SINUS and CHIRnMAG and the ERC starting grant NewHeavyFermion.

TABLE I. Table of uniaxial pressure dependencies along the a- and the c-axis, the corresponding normalized pressure dependencies in units of GPa^{-1} and the Grüneisen parameters.

	$\gamma_n = 102$ mJ mol^{-1}K^{-2} [18]	$T_c = 3.45$ K	$\chi^a = 4.1 \times 10^{-4}$[18]	$\chi^c = 3.2 \times 10^{-4}$[18]	$H_c^a = 0.72$ T

	$d\gamma_n/dp_i$ [mJ mol^{-1}K^{-2}GPa^{-1}]	dT_c/dp_i [K GPa^{-1}]	$d\chi^a/dp_i$ [GPa^{-1}]	$d\chi^c/dp_i$ [GPa^{-1}]	dH_c^a/dp_i [T GPa^{-1}]
a-axis	-7.74	-1.92	-1.43×10^{-5}	4.13×10^{-6}	-0.049
c-axis	-4.81	2.10	-6.74×10^{-6}	-3.08×10^{-5}	0.046

	$1/\gamma_n \times d\gamma_n/dp_i$	$1/T_c \times dT_c/dp_i$	$1/\chi^a \times d\chi^a/dp_i$	$1/\chi^c \times d\chi^c/dp_i$	$1/H_c^a \times dH_c^a/dp_i$
a-axis	-0.076	-0.56	-0.035	0.013	-0.709
c-axis	-0.047	0.61	-0.016	-0.096	0.664
volume	-0.199	-0.51	-0.086	-0.070	-0.754

Grüneisen parameter	$dln\gamma_n/dlnV$	$dlnT_c/dlnV$	$dln\chi^a/dlnV$	$dln\chi^c/dlnV$	$dlnH_c^a/dlnV$
volume	-8.9	-22.9	-3.9	-3.1	-33.9

[1] D. C. Johnston, Advances in Physics **59**, 803 (2010).

[2] J. Paglione and R. L. Greene, Nature Physics **6**, 645 (2010).

[3] G. R. Stewart, Rev. Mod. Phys. **83**, 1589 (2011).

[4] I. I. Mazin and J. Schmalian, Physica C: Superconductivity **469**, 614 (2009).

[5] H. Fukazawa, Y. Yamada, K. Kondo, T. Saito, Y. Kohori, K. Kuga, Y. Matsumoto, S. Nakatsuji, H. Kito, P. M. Shirage, K. Kihou, N. Takeshita, C.-H. Lee, A. Iyo, and H. Eisaki, Journal of the Physical Society of Japan **78**, 083712 (2009).

[6] T. Terashima, M. Kimata, H. Satsukawa, A. Harada, K. Hazama, S. Uji, H. Harima, G.-F. Chen, J.-L. Luo, and N.-L. Wang, Journal of the Physical Society of Japan **78**, 063702 (2009).

[7] M. Rotter, M. Tegel, and D. Johrendt, Physical Review Letters **101**, 107006 (2008).

[8] P. Popovich, A. V. Boris, O. V. Dolgov, A. A. Golubov, D. L. Sun, C. T. Lin, R. K. Kremer, and B. Keimer, Phys. Rev. Lett. **105**, 027003 (2010).

[9] Z. Li, D. L. Sun, C. T. Lin, Y. H. Su, J. P. Hu, and G.-q. Zheng, Phys. Rev. B **83**, 140506 (2011).

[10] R. Thomale, C. Platt, W. Hanke, J. Hu, and B. A. Bernevig, Phys. Rev. Lett. **107**, 117001 (2011).

[11] K. Hashimoto, A. Serafin, S. Tonegawa, R. Katsumata, R. Okazaki, T. Saito, H. Fukazawa, Y. Kohori, K. Kihou, C. H. Lee, A. Iyo, H. Eisaki, H. Ikeda, Y. Matsuda, A. Carrington, and T. Shibauchi, Physical Review B **82**, 014526 (2010).

[12] J.-P. Reid, M. A. Tanatar, A. Juneau-Fecteau, R. T. Gordon, S. R. de Cotret, N. Doiron-Leyraud, T. Saito, H. Fukazawa, Y. Kohori, K. Kihou, C. H. Lee, A. Iyo, H. Eisaki, R. Prozorov, and L. Taillefer, Phys. Rev. Lett. **109**, 087001 (2012).

[13] K. Okazaki, Y. Ota, Y. Kotani, W. Malaeb, Y. Ishida, T. Shimojima, T. Kiss, S. Watanabe, C.-T. Chen, K. Kihou, C. H. Lee, A. Iyo, H. Eisaki, T. Saito, H. Fukazawa, Y. Kohori, K. Hashimoto, T. Shibauchi, Y. Matsuda, H. Ikeda, H. Miyahara, R. Arita, A. Chainani, and S. Shin, Science **337**, 1314 (2012).

[14] T. Terashima, M. Kimata, N. Kurita, H. Satsukawa, A. Harada, K. Hazama, M. Imai, A. Sato, K. Kihou, C.-H. Lee, H. Kito, H. Eisaki, A. Iyo, T. Saito, H. Fukazawa, Y. Kohori, H. Harima, and S. Uji, Physical Review Letters **104**, 259701 (2010).

[15] T. Sato, K. Nakayama, Y. Sekiba, P. Richard, Y.-M. Xu, S. Souma, T. Takahashi, G. F. Chen, J. L. Luo, N. L. Wang, and H. Ding, Phys. Rev. Lett. **103**, 047002 (2009).

[16] C. H. Lee, K. Kihou, H. Kawano-Furukawa, T. Saito, A. Iyo, H. Eisaki, H. Fukazawa, Y. Kohori, K. Suzuki, H. Usui, K. Kuroki, and K. Yamada, Phys. Rev. Lett. **106**, 067003 (2011).

[17] J.-P. Castellan, S. Rosenkranz, E. A. Goremychkin, D. Y. Chung, I. S. Todorov, M. G. Kanatzidis, I. Eremin, J. Knolle, A. V. Chubukov, S. Maiti, M. R. Norman, F. Weber, H. Claus, T. Guidi, R. I. Bewley, and R. Osborn, Phys. Rev. Lett. **107**, 177003 (2011).

[18] F. Hardy, A. E. Böhmer, D. Aoki, P. Burger, T. Wolf, P. Schweiss, R. Heid, P. Adelmann, Y. Yao, G. Kotliar, J. Schmalian, and C. Meingast, ArXiv e-prints **1302.1696** (2013).

[19] L. de' Medici, G. Giovannetti, and M. Capone, ArXiv e-prints **1212.3966** (2012).

[20] F. Hardy, P. Adelmann, T. Wolf, H. v. Löhneysen, and C. Meingast, Physical Review Letters **102**, 187004 (2009).

[21] C. Meingast, F. Hardy, R. Heid, P. Adelmann, A. Böhmer, P. Burger, D. Ernst, R. Fromknecht, P. Schweiss, and T. Wolf, Physical Review Letters **108**, 177004 (2012).

[22] A. E. Böhmer, P. Burger, F. Hardy, T. Wolf, P. Schweiss, R. Fromknecht, H. v. Löhneysen, C. Meingast, H. K. Mak, R. Lortz, S. Kasahara, T. Terashima, T. Shibauchi, and Y. Matsuda, Physical Review B **86**, 094521 (2012).

[23] C. Meingast, B. Blank, H. Bürkle, B. Obst, T. Wolf, H. Wühl, V. Selvamanickam, and K. Salama, Physical Review B **41**, 11299 (1990).

[24] H. Fukazawa, T. Saito, Y. Yamada, K. Kondo, M. Hirano, Y. Kohori, K. Kuga, A. Sakai, Y. Matsumoto, S. Nakatsuji, K. Kihou, A. Iyo, C. H. Lee, and H. Eisaki, Journal of the Physical Society of Japan **80SA**, SA118 (2010).

[25] J. S. Kim, E. G. Kim, G. R. Stewart, X. H. Chen, and

X. F. Wang, Phys. Rev. B **83**, 172502 (2011).

[26] V. Grinenko, S.-L. Drechsler, M. Abdel-Hafiez, S. Aswartham, A. U. B. Wolter, S. Wurmehl, C. Hess, K. Nenkov, G. Fuchs, D. V. Efremov, B. Holzapfel, J. van den Brink, and B. Büchner, physica status solidi (b) (2013).

[27] M. Abdel-Hafiez, S. Aswartham, S. Wurmehl, V. Grinenko, C. Hess, S. L. Drechsler, S. Johnston, A. U. B. Wolter, B. Büchner, H. Rosner, and L. Boeri, Physical Review B **85**, 134533 (2012).

[28] C. Paulsen, D. Aoki, G. Knebel, and J. Flouquet, Journal of the Physical Society of Japan **80**, 053701 (2011).

[29] A. M. Clogston, Phys. Rev. Lett. **9**, 266 (1962).

[30] D. Zocco, "in preparation,".

[31] F. Hardy, "in preparation,".

[32] P. Ehrenfest, Mitteilungen aus dem Kammerlingh Onnes-Institut Leiden **75b**, 628 (1938).

[33] S. L. Bud'ko, Y. Liu, T. A. Lograsso, and P. C. Canfield, Phys. Rev. B **86**, 224514 (2012).

[34] D. Shoenberg, *Superconductivity* (Cambridge University Press, 1962).

[35] G. Brändli and F. D. Enck, Physics Letters A **26**, 360 (1968).

[36] P. Popovych, *Magnetostriction and Thermal Expansion of the High-Temperature Superconductor* $YBa_2Cu_3O_7$, Ph.D. thesis, Universität Karlsruhe (TH) (2006).

[37] R. Heid, "unpublished,".

[38] J. Flouquet, J. Brison, K. Hasselbach, L. Taillefer, K. Behnia, D. Jaccard, and A. de Visser, Physica C: Superconductivity **185 - 189, Part 1**, 372 (1991).